

Linear arrays of Josephson junctions: A stability analysis of characteristic modes

B. R. Trees

Department of Physics and Astronomy, Ohio Wesleyan University, Delaware, Ohio 43015

E. B. Harris*

Department of Physics, The Ohio State University, Columbus, Ohio 43210

(Received 28 July 1997)

We have performed a linear stability analysis of two arrays of resistively shunted Josephson junctions: a ladder array and a so-called modified linear array. We find the periodic solutions to be linearly stable for a wide range of bias currents in the absence of a load. This is contrasted with the well-studied globally coupled linear array, where stability of the periodic solutions is a sensitive function of bias current and load parameters. For the ladder array, we have studied the nature of the mesh currents for the different decay modes. Numerical evidence leads us to conclude that the branches of the ladder parallel to the bias current play an important role in helping to damp out perturbed currents. We also compare the long-time dynamics of these Josephson-junction arrays with that of an RL network, which is a ladder of resistors and inductors, and for which the decay rates and mesh currents are calculated exactly. We find that *at long times* the dynamics of all three arrays are basically identical. [S0163-1829(98)01809-8]

I. INTRODUCTION

The dynamics of linear arrays of N Josephson junctions globally coupled to a load of impedance Z has been of interest to researchers for basically two reasons: technological applications,^{1,2} and the opportunity to study a nonlinear system with many degrees of freedom.³⁻⁹ Of interest here have been periodic solutions in which the voltages across the junctions all oscillate with the same frequency and a fixed phase difference between neighboring junctions. The simplest of these, the so-called *in-phase* mode, corresponds to the case where phase differences between neighboring junctions is zero. The linear stability of this mode was found to be very sensitive to circuit parameters such as the bias current and the impedance of the load.^{4,5} (See the figures in Ref. 4 or 5.) From a numerical calculation of the Floquet exponents, Haldley, Beasley, and Wiesenfeld discovered that the *in-phase* mode is most stable with a McCumber parameter $\beta_c = 1$ and with bias currents of the order of the junction critical current.⁵ In the *splay-phase* mode, the voltages across neighboring junctions all have the same wave form but are shifted in time by T/N , where T is the period. A linear stability analysis indicated that this mode is neutrally stable (as indicated by a Floquet exponent of $+1$) in at least $N-2$ directions in the N -dimensional phase space of the system.⁶⁻⁹ The upshot here is that neither the *in-phase* nor *splay-phase* modes of the globally-coupled array show evidence of stability against perturbations for a wide range of circuit parameters.

Recently, Harris and Garland¹⁰ have studied a modified linear array (MLA) of Josephson junctions, as shown in Fig. 1. In this geometry, there are N junctions along the “backbone” of the array, $2(N-1)$ shunt junctions, which are parallel to the backbone and serve to couple pairs of backbone junctions, and $2N$ nodes, as shown in the figure. Bias currents of either I_B or $2I_B$ are injected and removed as shown. As is standard practice, one of the nodes of the circuit is

grounded, leaving a problem in which the superconducting phases at the $2(N-1)$ remaining nodes are to be calculated. Harris and Garland discovered that the total ac voltage across the backbone $V_{AB}(t)$ varied between zero and N times the ac voltage across a single junction, as a function of the size of the transverse magnetic field applied to the circuit. This was without a load connected to the circuit and so is a measure of the intrinsic behavior of the array. It was also discovered that the backbone voltage was quite robust to critical current disorder among the junctions.¹⁰

The goal of our work has been to understand as much as we can about the dynamics of the characteristic modes of the MLA and the ladder array. In Sec. II of this paper, we report the results of a Floquet analysis of the array, in which we demonstrate that, unlike in the globally coupled case, the periodic solutions are indeed linearly stable over a wide

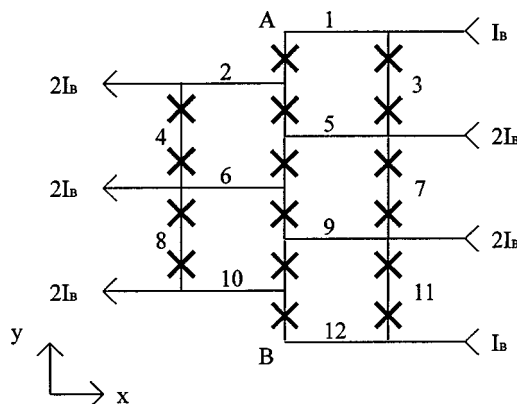


FIG. 1. Modified linear array (MLA) with six backbone junctions, $N=6$. All junctions parallel to the backbone are shunt junctions. Any applied magnetic fields are assumed uniform in the $+z$ direction. The numbers 1 through 12 label the nodes of the array, and so the voltage across the top junction in the backbone, for example, would be labeled $V_{1,2}$ as it is the difference in voltage between nodes 1 and 2. All junctions are resistively shunted.

range of bias currents. We also compare our results for the Floquet exponents with those of Harris and Garland, who performed a heuristic analysis of the stability of the solutions. In Sec. III we compare the dynamics of the MLA with that of a geometrically simpler ladder array of Josephson junctions, which allows us to study the physical distributions of currents corresponding to each of the characteristic modes of the system. (Each characteristic mode has its own Floquet exponent, although some exponents may be degenerate.) In Sec. IV we make a comparison between the MLA and a basic RL network,¹¹ for which an analytic result for the Floquet exponents is possible.

II. FLOQUET EXPONENTS FOR THE MLA

From Fig. 1 and conservation of charge, we can see that the current entering node j is given by

$$I_j = \sum_{\langle k \rangle} I_{c,jk} \sin(\phi_j - \phi_k + A_{jk}) + \frac{\Phi_0}{2\pi R_{jk}} \frac{d}{dt} (\phi_j - \phi_k), \quad (1)$$

where ϕ_j is the phase of the superconducting wave function at node j , I_j is the bias current entering node j , and the sum is over nodes that are connected to node j by a single junction. $I_{c,jk}$ is the critical current for the junction between nodes j and k ; for simplicity, we took all junctions to have the same critical current ($I_{c,jk} = 1.0 \mu\text{A}$). We worked within a resistively shunted-junction (RSJ) model, and so R_{jk} is the effective resistance of the junction between nodes j and k ; again, for simplicity we took all junctions to have the same resistance ($R_{jk} = 1.0 \text{ m}\Omega$). $\Phi_0 = h/2e$ is the flux quantum, and A_{jk} is the line integral of the vector potential between nodes j and k :

$$A_{jk} = \frac{2\pi}{\Phi_0} \int_j^k \mathbf{A} \cdot d\mathbf{l}.$$

All applied magnetic fields were taken to be uniform in the z direction, $\mathbf{B} = B\hat{z}$, which corresponds to a vector potential of $\mathbf{A} = Bx\hat{y}$. We solved Eq. (1) numerically for the phases $\phi_j(t)$ using a fourth-order Runge-Kutta algorithm. The time steps were taken to be approximately $0.002t_c$, where t_c is the characteristic time scale of a single junction, $t_c = \Phi_0/I_c R$.

For the stability analysis, suppose that $\phi_{0j}(t)$ is a solution to Eq. (1), found numerically by iterating the Runge-Kutta algorithm for many time steps. (Typically, we would run the program for at least 500 000 time steps.¹²) Then, we perturb the solution by a small amount, $\eta_j(t)$, so that the new phase at node j is $\phi_j(t) = \phi_{0j}(t) + \eta_j(t)$. Linearizing Eq. (1) with respect to η_j , we arrive at the following:

$$0 = \sum_{\langle k \rangle} \left[I_{c,jk} \cos(\phi_{0j} - \phi_{0k} + A_{jk})(\eta_j - \eta_k) + \frac{\Phi_0}{2\pi R_{jk}} \frac{d}{dt} (\eta_j - \eta_k) \right]. \quad (2)$$

Equation (2) is solved numerically for $\eta_j(t)$. On an intuitive level, we know that if the perturbations decay with time, the original solution $\phi_{0j}(t)$ is linearly stable. Of course, the for-

TABLE I. Floquet multipliers μ and the corresponding exponents λ for the modified linear array with $N=8$, $f=1/2$ and $I_B/I_c=8$. The multiplier equal to one reflects the neutral stability of the system when perturbed along a direction tangential to the periodic orbit. We are mostly interested in the next row of the table, which gives the multiplier and exponent for the longest-lived mode of the array. Note the seven nearly degenerate multipliers, which correspond to physically similar, rapidly decaying modes.

| μ | $\lambda t_c = \ln(\mu)/(T/t_c)$ |
|--------|----------------------------------|
| 0.9999 | -8.0×10^{-4} |
| 0.9458 | -0.444 |
| 0.8366 | -1.423 |
| 0.7405 | -2.396 |
| 0.6746 | -3.140 |
| 0.6332 | -3.645 |
| 0.6085 | -3.962 |
| 0.5953 | -4.137 |
| 0.4560 | -6.264 |
| 0.4560 | -6.264 |
| 0.4559 | -6.265 |
| 0.4559 | -6.265 |
| 0.4559 | -6.265 |
| 0.4559 | -6.265 |
| 0.4559 | -6.265 |

malism of Floquet analysis gives us a mathematically rigorous method for determining stability.¹³ We look for solutions of the form

$$\eta_j(t+T) = \mu \eta_j(t), \quad (3)$$

where T is the period to the solution of Eq. (1) and μ is called the Floquet multiplier. If $\mu > 1$, the perturbations grow with time, and if $\mu < 1$ the perturbations diminish with time. The special case of $\mu = 1$ corresponds to a neutrally stable solution. An array with N backbone junctions, will have $2N-1$ nodes and thus it will yield $2N-1$ multipliers. At least one of these multipliers must equal one; in the language of phase space, this corresponds to a perturbation tangent to the periodic orbit.

As discussed in Ref. 8 we find the Floquet multipliers of our system as follows. We perturb in one direction in phase space, that is, we start with $\eta_j = 1$ and $\eta_k = 0$ ($k \neq j$). We use the Runge-Kutta algorithm to find the values of η_k and all the η_j one period later. These $2N-1$ quantities then constitute one column of a $(2N-1) \times (2N-1)$ matrix, the other columns coming from perturbing the solution at a different value of j . The eigenvalues of the resulting matrix will then be the Floquet multipliers of the system.¹⁴

We calculated the multipliers for arrays with varying N . (The largest array had 30 backbone junctions.) We also varied the bias current, allowing for values of $I_B/I_c = 2$ and $I_B/I_c = 8$, the latter being too large for the globally coupled array to exhibit stable solutions. Lastly, we allowed for either zero external magnetic field, or a field characterized by a frustration parameter of $f = 1/2$ or $f = 1/3$, where $f = BS/\Phi_0$, and S is the area of a cell (a cell being formed by two backbone and two shunt junctions). For example, Table I shows all the Floquet multipliers for the MLA with $N=8$,

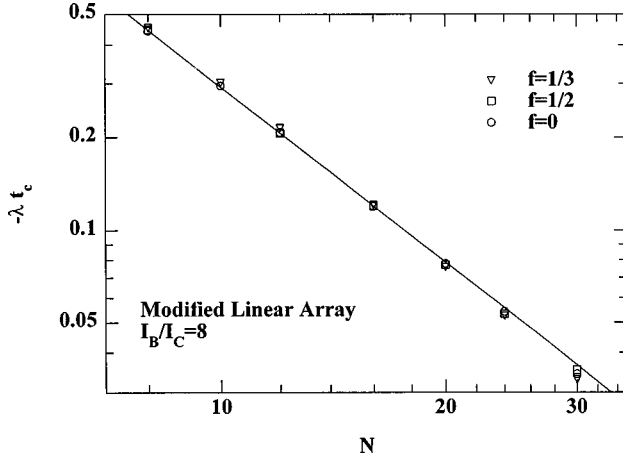


FIG. 2. Floquet exponents for the MLA as a function of the number of backbone junctions. The line is a linear regression fit to the $f=0$ case and has a slope of -1.99 . The plot shows that the same exponents occur for magnetic fields corresponding to $f=1/2$ and $f=1/3$. In all three cases the exponents depend on array size according to $\lambda \sim 1/N^2$.

$f=1/2$, and $I_B/I_c=8$. The seven smallest multipliers are nearly degenerate and correspond to a characteristic mode of the array that quickly decays. The longest lived mode, with $\mu=0.9458$, is of interest, since physically that mode would dominate the long-time behavior of the array. From Eq. (3), we see that this multiplier corresponds to a mode that decays by 5.42% in one period, while the most rapidly decaying mode decays by 54% in the same amount of time. Table I also displays the Floquet exponents, λ , where the exponent is related to the multiplier via $\mu = e^{\lambda T}$.

Figure 2 shows our results for the Floquet exponents as a function of N for $f=0$, $f=1/2$, and $f=1/3$. The solid line is a linear regression fit for the $f=0$ case and has a slope of -1.99 . Thus we see the same dependence on array size as reported by Harris and Garland. Namely, the Floquet exponents decrease with increasing array size according to $1/N^2$, as seen in diffusive transport problems.¹⁵ Effectively, as the array size grows, the mode exhibiting the longest time behavior takes longer to settle down when kicked away from equilibrium. This behavior is not observed in the globally coupled array, where the Floquet exponents showed no dependence on N .⁵ Figure 2 also clearly shows that the exponents show no significant variation with applied magnetic field, at least not for the values of f and I_B/I_c studied so far. Physically, we know that an external field will certainly affect the nature of the periodic solutions for the phases, ϕ_j , but apparently it does not affect how perturbations away from these solutions decay with time.

We have studied, numerically, how the perturbed phases $\eta_j(t)$ decay as a function of time for $I_B/I_c=8$. We observe an exponential decay with small-amplitude oscillations superimposed. In zero magnetic field, the period of the oscillations (which is a function of the bias current) is approximately 2.5 times shorter than the relaxation time characterizing the exponential decay. In the presence of an external magnetic field, the oscillations are shifted in phase (by an amount dependent on the value of the frustration parameter f), but the relaxation time is not affected. This latter behavior is consistent with field-independent Floquet multi-

pliers (as observed for bias currents of $I_B/I_c=2$ and greater). The physics underlying this behavior is under investigation.

We have studied the stability of the array for two bias currents, $I_B/I_c=8$ and $I_B/I_c=2$. Figure 3(a) shows that the Floquet multipliers are smaller for the smaller bias current. That is, for $I_B/I_c=2$ perturbations decay more in one period than for $I_B/I_c=8$. The period of the solutions, however, depends on the bias current via the expression¹⁶

$$\frac{T}{t_c} = \frac{2\pi}{\sqrt{(I_B/I_c)^2 - 1}}, \quad (4)$$

so it is also of interest to calculate the corresponding Floquet exponents, which follow from the expression

$$\lambda t_c = \frac{\ln \mu}{T/t_c}. \quad (5)$$

From Fig. 3(c), we see that the exponents are roughly the same for the two bias currents studied so far. Thus, from Eq. (5), we hypothesize that $\ln \mu$ has the same dependence on the bias current as does the period.¹⁷ Based on Fig. 3, we expect that the Floquet exponents are independent of bias current and thus the stability is independent of bias current.

III. COMPARISON OF MLA AND LADDER ARRAY

We have also studied the dynamics of the modes of a ladder array of Josephson junctions with the bias currents injected perpendicular to the long axis of the ladder. (See Fig. 4.) Numerical simulations show that those junctions perpendicular to the injected bias currents behave analogously to the shunt junctions in the MLA. See Ref. 10 for a discussion of the role of the shunt junctions in the MLA. Interestingly, we find that the dynamics driving the decay characteristics of the ladder are the same as for the MLA, since we find the same Floquet exponents for both types of arrays. (See Fig. 5, which shows results for $f=1/2$ and $I_B/I_c=8$.)

Furthermore, for a ladder of a given size we find it easier to comprehend physically the nature of the currents flowing for each of the decay modes than is the case for the MLA. To see what we mean, consider an array with seven cells (or meshes), which we label as $M=7$. There will be $2M+1=15$ Floquet multipliers, signifying 15 characteristic decay modes of the system. From Fig. 5, it should not be surprising that these multipliers agree with those in Table I to within 0.5%. Ignoring the case of a multiplier equal to unity, so far we have only discussed the multiplier corresponding to the slowest-decaying mode (in this case, $\mu=0.9458$). But now let us ask how the mesh currents flow around each of the cells for all of the 14 remaining multipliers in Table I. The currents are computed numerically for the ladder, by finding the eigenvectors of the $(2M+1) \times (2M+1)$ matrix, the formation of which is described in Sec. II. The components of the vectors give the values of the phases at the 14 nodes, and from these the perturbed currents flowing in each cell can be calculated.

First, consider the decay modes represented by the seven nearly degenerate Floquet multipliers. These are the most rapidly decaying modes. We have studied one of these in detail. Figure 6(a) shows that this mode corresponds to a situation where two nodes at the same y value experience

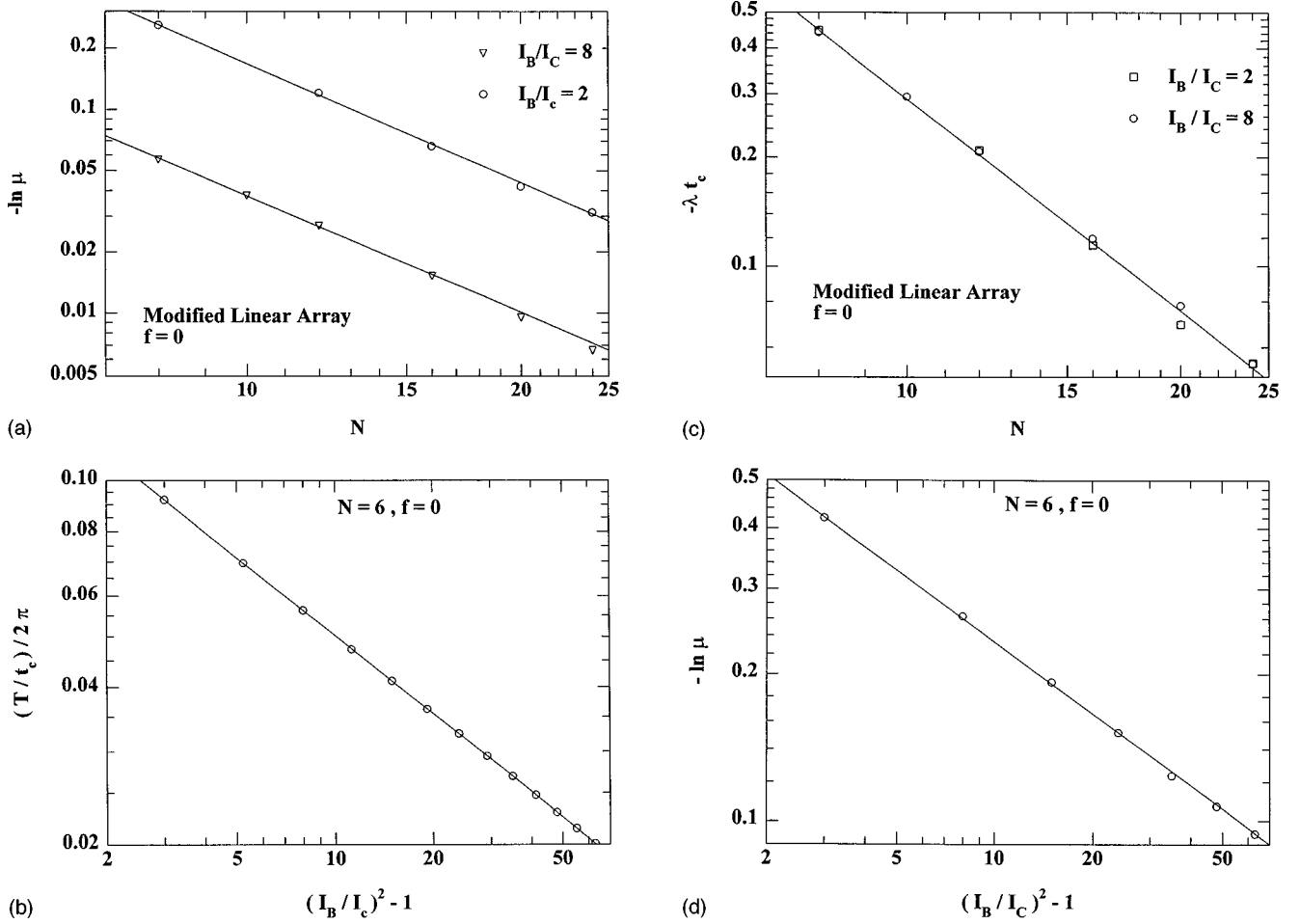


FIG. 3. (a) Natural logarithm of the Floquet multipliers for the MLA as a function of the number of backbone junctions. The two data sets correspond to bias currents of $I_B/I_c=8$ and $I_B/I_c=2$. It is clear that for the smaller bias current, perturbations will decay more in one period than for the larger bias current. (b) Period of the solutions to the MLA as a function of bias current for six backbone junctions and zero applied magnetic field. The straight line is a linear regression fit to the data points and has a slope of -0.5 , demonstrating the period and bias current are related by the expression $T/t_c = 2\pi/\sqrt{(I_B/I_c)^2 - 1}$. (c) Floquet exponents of the MLA as a function of the number of backbone junctions for the same bias currents as used in (a). This figure demonstrates that the *exponents* are independent of the bias currents, whereas (a) shows that the *multipliers* do depend on the bias current. This must mean that the multipliers and the period have the same dependence on bias current. [See (d).] (d) Natural logarithm of the Floquet multipliers of the MLA as a function of the bias current for six backbone junctions and zero applied magnetic field. The line is a linear regression fit to the data points and has a slope of -0.495 . This is numerical evidence that the logarithm of the multipliers and the period have the same dependence on bias current.

perturbed currents flowing into them from both directions along the ladder. If we define a vorticity of $+1$ (-1) for each cell in which the mesh currents flow clockwise (counterclockwise), and 0 otherwise, then two cells have a vorticity of zero. The overall ladder, in this mode, has a vorticity of -1 .

Now, consider the *next* fastest-decaying mode, with a multiplier of 0.5953 . Figure 6(b) shows that the decaying currents in this case all correspond to a well-defined clockwise or counterclockwise flow in each cell. Inspection of the figure shows that the mesh currents are arranged so as to maximize the amount of current flowing in the horizontal branches (x direction) of the ladder. We are lead to conjecture that large horizontal currents are a very effective way to damp out perturbations. An analysis of the currents for the multipliers ranging from 0.8366 to 0.5953 shows that all correspond to three clockwise and four counterclockwise mesh currents, or vice versa, with the slowest of these modes ($\mu=0.8366$) having only one horizontal branch where the

mesh currents from neighboring cells flow in the same direction. This is shown in Fig. 6(c).

Lastly, the slowest mode, which we focused on in Sec. II, is depicted in Fig. 6(d) and corresponds to seven clockwise mesh currents and a vorticity of $+7$. In this case, all horizontal branches have mesh currents from neighboring cells flowing in opposite directions. To generalize what we see in Fig. 6, the fastest nondegenerate mode is that with the highest spatial frequency in the flow direction of mesh currents, and the slowest mode has the lowest spatial frequency. Apparently, the slowest modes do not make effective use of the junctions in the horizontal branches of the ladder to help dissipate perturbed currents.

IV. COMPARISON OF MLA WITH RL NETWORK

An analytically tractable problem results if we replace the biased junctions (those parallel to the bias currents) of the ladder with resistors and the shunt junctions (those perpen-

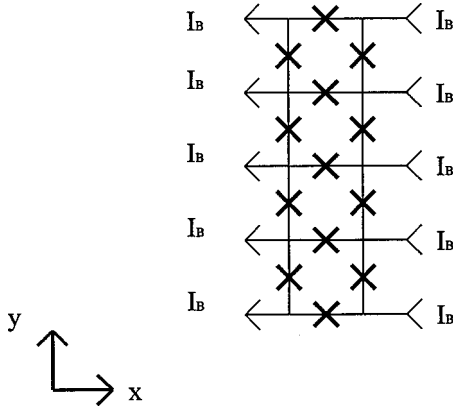


FIG. 4. Ladder array of resistively shunted Josephson junctions with four cells, or meshes, $M=4$. We calculate the phases at the nodes of the array and the bias currents are injected and removed parallel to the horizontal (x direction) branches.

dicular to the bias currents) with inductors. For the shunt junctions, this must be reasonable, since we know that they carry small currents, and for $I \ll I_c$ a junction behaves inductively, with an effective inductance of $\Phi_c/2\pi I_c$.¹⁸ The geometry is shown in Fig. 7. We find some interesting parallels between the two kinds of arrays, which we now discuss. We search for solutions for the mesh currents of the form

$$i_k = I_k e^{\lambda t}, \quad (6)$$

where k ranges from 1 to M and indexes the mesh currents. This is actually just a normal-mode problem,¹⁹ and so we

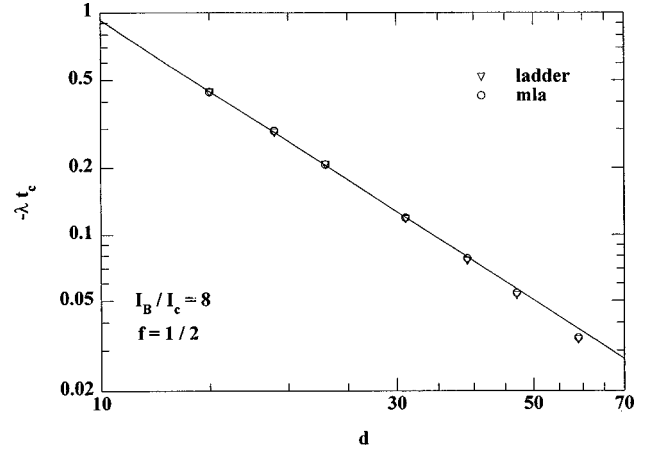


FIG. 5. Floquet exponents as a function of the effective dimensionality d of the MLA and the ladder array with $I_B/I_c=8$ and $f=1/2$. For the MLA, $d=2N-1$, and for the ladder array, $d=2M+1$, where N is the number of backbone junctions and M is the number of meshes. The plot shows that the dynamics of the longest-lived decay mode is the same for both geometries.

shall merely state our results. The characteristic decay rates and the currents I_k are given by

$$\lambda_n = -4 \left(\frac{R}{L} \right) \sin^2 \left[\frac{\pi n}{2(M+1)} \right]$$

where

$$n = 1, 2, \dots, M, \quad (7)$$

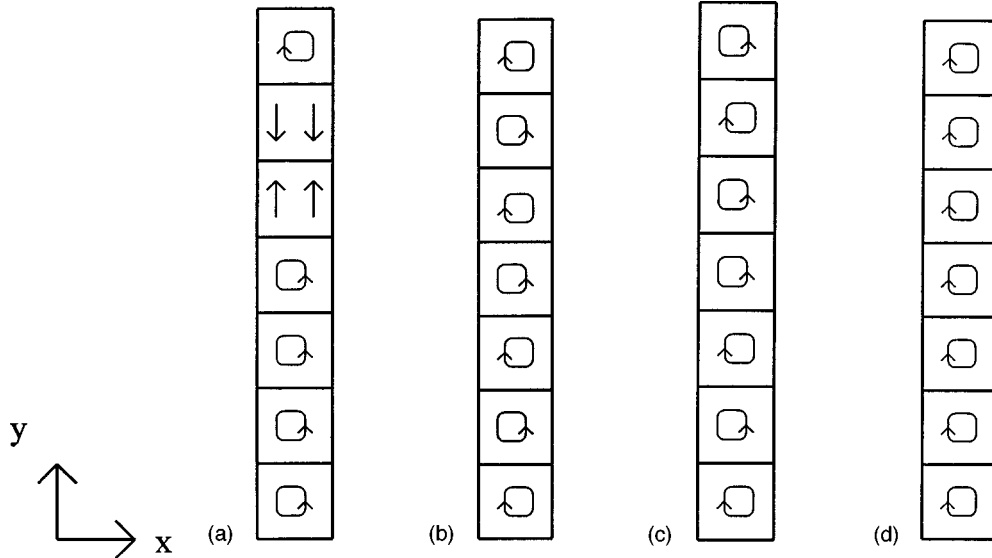


FIG. 6. This figure characterizes the perturbed currents for four of the 15 decay modes in a ladder array with seven meshes in the absence of an external magnetic field. In (a), the mode depicted has a Floquet multiplier of $\mu=0.4559$ and is one of seven similar, rapidly decaying modes. Note that two of the cells do not have a well-defined vorticity. Taking clockwise (counterclockwise) mesh currents to have a vorticity of $+1$ (-1), this mode corresponds to an array with total vorticity of -1 . (b) corresponds to $\mu=0.5953$ and is the next fastest decaying mode after that shown (a). The current in each cell has a well-defined vorticity, and in fact the currents are arranged so as to maximize the number of horizontal branches in which the currents from neighboring cells flow in the same direction. (c) corresponds to $\mu=0.8366$ and is the next to slowest decaying mode. The mesh currents now are arranged so as to have only one horizontal branch through which the currents from neighboring cells flow in the same direction. (d) corresponds to $\mu=0.9458$ and depicts the slowest decaying mode. The array has a total vorticity of $+7$ and clearly minimizes the amount of current flowing through the horizontal branches. (b)–(d) demonstrate that the horizontal branches (analogous to the shunt junctions of the MLA) are important in those modes where perturbations are more rapidly damped out.

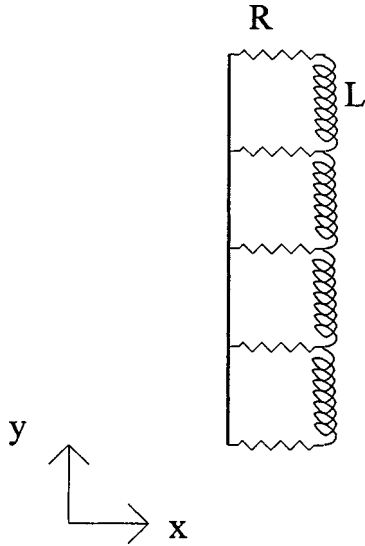


FIG. 7. An RL ladder array. For comparison with the ladder array of Josephson junctions the shunt junctions have been replaced by inductors and the biased junctions have been replaced by resistors. Note that there is one inductor and two resistors per cell.

$$I_k^{(n)} = \begin{cases} I, & k=1 \\ I \frac{\sin[k\pi n/(M+1)]}{\sin[\pi n/(M+1)]}, & 2 \leq k \leq M-1 \\ I \frac{\sin[(M-1)\pi n/(M+1)]}{\sin[2\pi n/(M+1)]}, & k=M, \end{cases} \quad (8)$$

where I is an arbitrary current. In Eqs. (7) and (8), n indexes the normal modes. In this work, we have been most interested in the slowest decay mode, which corresponds to $n=1$ for a given array size. Interestingly, when we compare the decay rate for the RL network using Eq. (7) with the numerically obtained Floquet exponent for the MLA for a given array size, we get excellent agreement.²⁰ This is demonstrated in Fig. 8. It seems that the long-time dynamics of the MLA and the RL network indeed are the same.

Another benefit of looking at the RL network, is that using Eqs. (7) and (8), it is possible to reproduce analytically the same behavior we saw from the numerical study of the ladder array of Josephson junctions. Namely, the fastest-decaying mode in the RL network corresponds to mesh currents in neighboring cells flowing in opposite senses, while the slowest-decaying mode means the currents are all flowing in the same sense, again pointing to the fact that currents in the horizontal branches are effective at returning a perturbed array to equilibrium. Given the observed similarity in the dynamics of the RL and ladder arrays, the result is of more than just passing interest. For the mathematical details see the Appendix.

V. CONCLUSIONS

We have studied the stability of the periodic solutions to three linear arrays: the modified linear array of Josephson junctions, the ladder of Josephson junctions, and a ladder array of resistors and inductors. We find the long-time dynamics that drives the systems back to equilibrium when perturbed are all identical, as evidenced by approximately

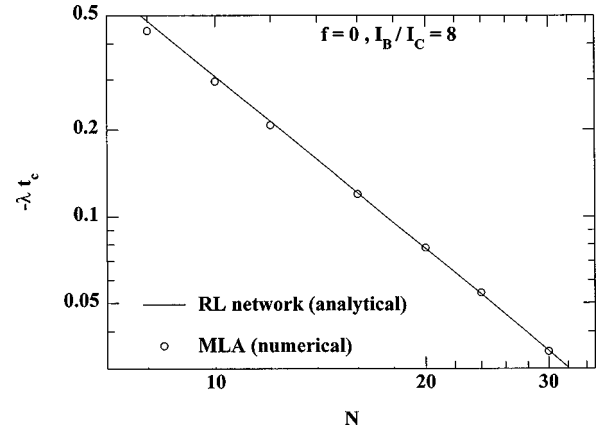


FIG. 8. Comparison of the Floquet exponents, as calculated numerically for the MLA, and the decay rates, as calculated analytically for the RL network, as a function of the number of backbone junctions (for the MLA) or the number of cells (for the RL network). For a given N we are looking at only the longest-lived mode. The agreement is surprisingly good.

numerically equal Floquet exponents. We also discover a dependence on the Floquet exponents with array size that is similar to that observed in diffusive transport problems, as reported previously.¹⁰ For the ladder of Josephson junctions we were able to characterize numerically the nature of the decay modes and found that the fastest-decaying mode corresponds to neighboring cells with opposite flowing mesh currents, while the slowest mode corresponded to cells with all mesh currents flowing in the same sense, leading us to conclude that currents in the horizontal branches of the ladder (parallel to the direction of the injected bias currents) are efficient at damping out perturbations. Lastly, we were able to calculate the Floquet exponents and decay currents for a “simple” RL ladder and compare them with the results for the MLA. We find identical *long-time* behavior for both circuits, indicating that, once perturbed, the same dynamics drive the linearized Josephson arrays and the linear RL ladder back to their steady-state behavior.

ACKNOWLEDGMENTS

The authors wish to thank David Stroud for helpful conversations. For part of this work, E.B.H. was supported by NSF Grant No. DMR-9501272 and by DOE (MISCON) through Contract No. DE-FG02-90ER45427.

APPENDIX

In this appendix we want to note two of the consequences of Eqs. (7) and (8). First, consider the mode with the fastest decay rate, corresponding to $n=M$. We want to show that this represents mesh currents in neighboring cells that flow in opposite senses. In Eq. (8) we can take $I>0$, corresponding to a clockwise mesh current in the first cell. Next, consider cells 2 through $M-1$. The sign of the currents follows from the expression

$$\frac{\sin[k\pi M/(M+1)]}{\sin[\pi M/(M+1)]}. \quad (A1)$$

Clearly, the denominator is positive, since the argument of the sine function is greater than 0 but less than π . The numerator will in fact alternate in sign as k steps through its allowed values as long as

$$(k-1)\pi < \frac{k\pi M}{M+1} < k\pi,$$

which is equivalent to the requirement that $k < M+1$. Since the largest value of k is $k=M$, this inequality is indeed satisfied. Thus, for $I > 0$, the current in the second cell flows counterclockwise; the current in the third cell flows clockwise, etc. up through cell $M-1$. It remains to show that the current in the last cell (with $k=M$) flows oppositely to the current in cell $M-1$. From Eqs. (8) and (A1) we see that both expressions for I_{M-1} and I_M have the same numerator. The denominator for I_{M-1} is shown above. In the expression for I_M , the denominator is

$$\sin[2\pi M/(M+1)].$$

Now we see that the denominators of the expressions for these two currents are of opposite signs for all values of $M > 1$, and since they have identical numerators, the currents

themselves have opposite signs. Thus we have demonstrated, that the fastest-decaying mode of the RL network corresponds to mesh currents flowing in alternating senses.

Next, consider the mode with the slowest time constant, corresponding to $n=1$. We want to show that in this case all the mesh currents will flow in the same sense. Again, take $I > 0$. For $2 \leq k \leq M-1$ the currents are given by

$$\frac{\sin[k\pi/(M+1)]}{\sin[\pi/(M+1)]}.$$

Clearly both the denominator and numerator are positive, since their arguments are between 0 and π . So all of these currents flow in a clockwise sense, as in the first cell. It remains to check the current in the last cell, for which

$$I_M = \frac{\sin[(M-1)\pi/(M+1)]}{\sin[2\pi/(M+1)]}.$$

The arguments of both sine functions are less than π for any $M > 1$, thus $I_M > 0$, and the current in the last cells flows clockwise. Thus we have shown that the slowest mode of the RL network corresponds to mesh currents all flowing in the same sense.

*Permanent address: Lucent Technologies, Orlando, FL.

¹A. K. Jain, K. K. Likharev, J. E. Lukens, and J. E. Sauvageau, *Phys. Rep.* **109**, 310 (1984).

²J. B. Hansen and P. E. Lindelof, *Rev. Mod. Phys.* **56**, 431 (1984).

³S. Watanabe and S. H. Strogatz, *Physica D* **74**, 197 (1994).

⁴P. Hadley and M. R. Beasley, *Appl. Phys. Lett.* **50**, 621 (1987).

⁵P. Hadley, M. R. Beasley, and K. Wiesenfeld, *Phys. Rev. B* **38**, 8712 (1988).

⁶K. Y. Tsang, R. E. Mirollo, S. H. Strogatz, and K. Wiesenfeld, *Physica D* **48**, 102 (1991).

⁷K. Y. Tsang and I. B. Schwartz, *Phys. Rev. Lett.* **68**, 2265 (1992).

⁸S. Nichols and K. Wiesenfeld, *Phys. Rev. A* **45**, 8430 (1992).

⁹S. H. Strogatz and R. E. Mirollo, *Phys. Rev. E* **47**, 220 (1993).

¹⁰E. B. Harris and J. C. Garland, *Phys. Rev. B* **55**, 3832 (1997).

¹¹For a brief description of a similar resistive-capacitive network, see P. M. Chaiken and T. C. Lubensky, *Principles of Condensed Matter Physics* (Cambridge University Press, New York, 1995), p. 381.

¹²There are known algorithms for calculating the solutions to periodic, steady-state systems. See, for example, K. S. Kundert, J. K. White, and A. Sangiovanni-Vincentelli, *Steady-State Methods for Simulating Analog and Microwave Circuits* (Kluwer Academic, Boston, 1990).

¹³Steven Strogatz, *Nonlinear Dynamics and Chaos* (Addison-Wesley, Reading, MA, 1994), p. 281.

¹⁴For a mathematical proof see, for example, D. W. Jordan and P. Smith, *Nonlinear Ordinary Differential Equations* (Clarendon, Oxford, 1977), pp. 231–234.

¹⁵For a discussion of diffusion on a lattice and in an RC network, see Ref. 11.

¹⁶We have checked numerically and found this relation to be well followed for $N=6$. See Fig. 3(b).

¹⁷Again, for $N=6$ we have shown numerically that this is accurate. See Fig. 3(d).

¹⁸T. van Duzer and C. W. Turner, *Principles of Superconducting Devices and Circuits* (Elsevier, New York, 1981), p. 185.

¹⁹The interested reader should consult, for example, A. Fetter and J. Walecka, *Theoretical Mechanics of Particles and Continua* (McGraw-Hill, New York, 1980), pp. 108–115.

²⁰Some care must be taken in a quantitative comparison of the RL ladder with the MLA. The number of meshes M and the number of backbone junctions of the MLA, N , are related by $M+1=N$. Furthermore, because there are two shunt junctions per cell of the MLA and only one inductor per cell of the RL ladder, Eq. (8) must be divided by two to compare with the MLA. Lastly, we make the change of variables L/R with $t_c/2\pi$.